Heliyon 9 (2023) e18136

Contents lists available at ScienceDirect

Heliyon

journal homepage: www.cell.com/heliyon

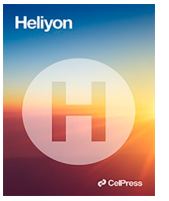

Necroptosis-related signatures identify two distinct hepatocellular carcinoma subtypes: Implications for predicting drug sensitivity and prognosis

Hui Tang [a,1], Caixia Qiao [b,1], Zhenwei Guo [c], Ruixuan Geng [d], Zhao Sun [a], Yingyi Wang [a,*], Chunmei Bai [a]

[a] *Department of Medical Oncology, Peking Union Medical College Hospital, Chinese Academy of Medical Sciences & Peking Union Medical College, Beijing, China*
[b] *Department of Medical Oncology, Liaocheng Third People's Hospital, Liaocheng, China*
[c] *Department of Clinical Laboratory, Liaocheng Third People's Hospital, Liaocheng, China*
[d] *Department of International Medical Services, Peking Union Medical College Hospital, Chinese Academy of Medical Sciences & Peking Union Medical College, Beijing, China*

ARTICLE INFO

Keywords:
Necroptosis
Liver cancer
Prognostic evaluation
Drug sensitivity
Molecular subtype

ABSTRACT

Background: Necroptosis is associated with oncogenesis, tumor immunity and progression. This research aims to investigate the association of necroptosis-related genes with drug sensitivity and prognosis in hepatocellular carcinoma (HCC).
Methods: Based on necroptosis-related signatures, HCC patients retrieved from the TCGA database were categorized. Survival outcomes, mutation profile, immune microenvironment, and drug sensitivity between HCC subtypes were further compared. Then, LASSO analysis was performed to construct a necroptosis-related prognostic signature, which was further evaluated using another independent cohort.
Results: A total of 371 patients with HCC could be categorized into two necroptosis-related subtypes. About 36% of patients were allocated to subtype A, with worse survival, more mutant TP53, and a lower likelihood of immunotherapy response. In contrast, patients in subtype B had a favorable prognosis, with lower expression of immunosuppressive signatures but a lower abundance of B and $CD8^+$ T-cell infiltration. The prognostic risk score calculated using the expression levels of nine genes involved in the necroptosis pathway (MLKL, FADD, XIAP, USP22, UHRF1, CASP8, RIPK3, ZBP1, and FAS) showed a significant association with tumor stage, histologic grade, and Child–Pugh score. Additionally, the risk score model was proven to be accurate in both the training and independent external validation cohorts and performed better than the TNM staging system and three well-recognized risk score models.
Conclusions: Based on necroptosis-related signatures, we identified two HCC subtypes with distinctive immune microenvironments, mutation profiles, drug sensitivities, and survival outcomes. A novel well-performing prognostic model was further constructed.

* Corresponding author. Department of Medical Oncology, Peking Union Medical College Hospital, Chinese Academy of Medical Sciences and Peking Union Medical College, Beijing, China.
E-mail address: wangyingyi@pumch.cn (Y. Wang).
[1] These authors contributed equally to this work.

https://doi.org/10.1016/j.heliyon.2023.e18136
Received 9 February 2023; Received in revised form 3 July 2023; Accepted 8 July 2023
Available online 11 July 2023

1. Introduction

Hepatocellular carcinoma (HCC) is a common cancer and the fourth leading cause of tumor-related death [1]. Approximately 70% of patients relapse within 5 years after HCC resection, while the median overall survival (OS) of advanced HCC patients is approximately 1 year [1,2]. Due to HCC heterogeneity and the influence of nontumor factors, it is difficult to precisely evaluate the survival outcome by TNM staging alone. Furthermore, there is no reliable measure to predict drug sensitivity that can aid in clinical decision-making. Hence, further research on the mechanisms of HCC tumorigenesis and progression is needed, which will facilitate the discovery of novel prognostic indicators and therapeutic targets.

In contrast to apoptosis, necroptosis is programmed necrotic cell death independent of caspase and was first identified in 2005 [3]. Necroptosis has been linked to hepatic inflammation, regeneration, fibrogenesis, and cancers [4–7]. Accumulating evidence has suggested that necroptosis and necroptosis-related genes are associated with tumorigenesis, sensitivity to drug therapy, and prognosis in HCC patients [8–11]. Therefore, patient classification and risk score in HCC based on necroptosis-related signatures (mRNA expression levels) can help to identify patient characteristics, guide clinical decisions and predict prognosis. Nevertheless, the effect of necroptosis-related signatures on HCC classification has not been estimated.

In this research, according to necroptosis-related signatures, HCC patients retrieved from The Cancer Genome Atlas (TCGA) database were assigned to different molecular subgroups. Then, the association of molecular subgroups with clinicopathological characteristics, prognosis, mutation profile, immune microenvironment, and drug sensitivity was further investigated. Moreover, a novel necroptosis-related prognostic model was established and estimated.

2. Methods

2.1. Data sources and processing

The mRNA expression, somatic mutation profiles, and clinical data of HCC samples were downloaded from the TCGA database (https://portal.gdc.cancer.gov/) in February 2022. International Cancer Genome Consortium (ICGC) (https://dcc.icgc.org/) HCC cohorts (ICGC-LIRI) were retrieved for external validation. To lower statistical bias, the transcripts per kilobase million (TPM) format was adopted for mRNA expression data [12]. HCC patients without complete follow-up data were excluded from the survival analysis.

2.2. Consensus clustering analysis

Based on previous publications [4,13–17], 18 necroptosis-related key genes were retrieved and are listed in Supplementary Table S1. The TCGA-LIHC cohort was divided into different molecular subtypes based on necroptosis-related gene expression by the R package "ConsensusClusterPlus" for consensus unsupervised clustering analysis [18]. The optimum number of subgroups was determined according to the following criteria: After categorization, the intercluster correlation decreased, but the intracluster correlation increased. Meanwhile, the cumulative distribution function (CDF) curve rose steadily. Finally, none of the subtypes had a sample size that was too small. Furthermore, using the R package "Rtsne" [19], *t*-SNE analysis was applied to validate the accuracy of this classification.

2.3. Evaluating the differences in HCC patients among molecular subtypes

Kaplan–Meier curves were utilized to compare the difference in survival time between distinct subgroups. The 20 most commonly mutated genes were identified by the R package "maftools" [20]. A Perl script was utilized to compute tumor mutation burden (TMB). The data on tumor-infiltrating cell abundance in the TCGA-LIHC cohort were downloaded from the xCell program [21]. xCell is a validated tool to conduct immune cell type analysis from transcriptome data. When screening differentially expressed genes between different subtypes, an adjusted p value < 0.05 and $|\log2\text{-fold change (FC)}| > 1$ were set as the cutoff. The R packages "clusterProfiler", "org.Hs.eg.db", and "enrichplot" were used to conduct Kyoto Encyclopedia of Genes and Genomes (KEGG) and Gene Ontology (GO) enrichment analyses [22].

2.4. Drug sensitivity analysis

Immune checkpoint inhibitor (ICI) therapy responses were predicted by Tumor Immune Dysfunction and Exclusion (TIDE) [23] by assessing immune evasion signatures. After uploading the transcriptome data, predicted immunotherapy responses and TIDE scores can be retrieved, and a lower TIDE score means a higher likelihood of immunotherapy response. The Genomics of Drug Sensitivity in Cancer (GDSC) algorithm [24] and R package "pRRophetic" [25] were employed to compute the half-maximal inhibitory concentration (IC50) of chemotherapy or targeted drugs.

2.5. Development of the necroptosis-related prognostic model

Least absolute shrinkage and selection operator (LASSO) analysis was employed by the R package "glmnet" [26] to select potent independent prognostic genes from necroptosis-related signatures. Nine necroptosis-related genes were selected to build the risk

signature based on the optimal lambda identified by 10-fold cross-validation and "one-standard error (1 se)". The necroptosis-based risk score was calculated in the following way: Risk score = ∑(exp GeneN × coef GeneN).

2.6. Estimation of the prognostic model

HCC patients were allocated to the high- or low-risk group according to necroptosis-related risk scores and the optimum OS cutoff generated by the R package "survminer". Likewise, the formula and cutoff were utilized to determine the risk scores for patients in an external ICGC cohort. Cox regression analysis was employed to retrieve the 95% confidence intervals (CI) and hazard ratios (HR) of variables. Then, a nomogram was developed and evaluated by the calibration curve and receiver operating characteristic (ROC) curve. After that, decision curve analysis (DCA) was performed to compare the prognostic accuracy of TNM staging and the nomogram model.

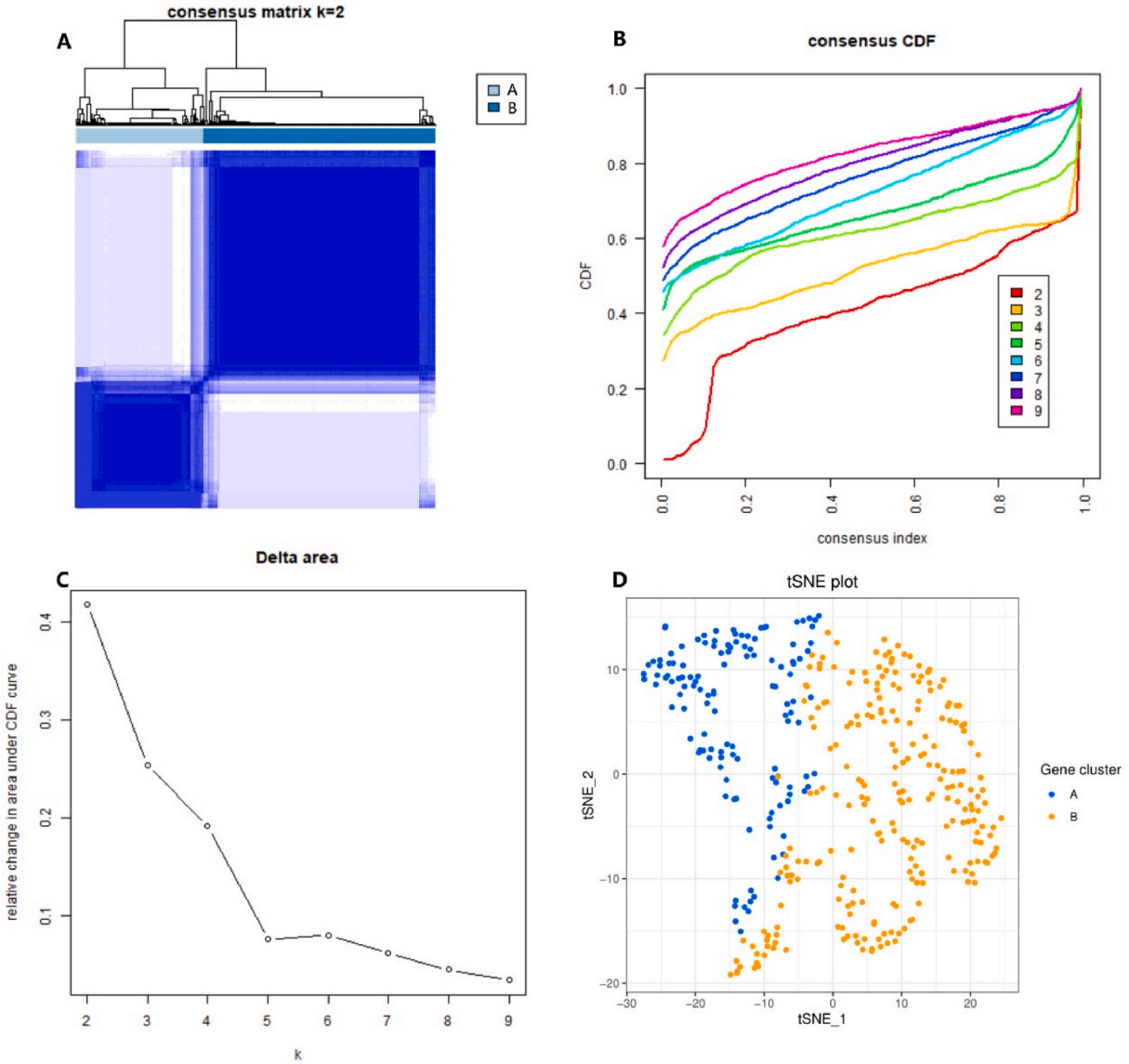

Fig. 1. Consensus clustering analysis in patients with hepatocellular carcinoma based on necroptosis-related genes. (A) HCC patients were divided into two subtypes based on the consensus clustering matrix (k = 2). (B) CDF of cluster result. (C) Delta area of cluster result. (D) *t*-SNE analysis based on necroptosis-related signatures. CDF, cumulative distribution function. CDF plots display consensus distributions for each k. Delta area plot displays the relative change of the area under the CDF curve between each k and k-1. The larger the value, the more obvious the improvement of the clustering effect under this k value is compared with that of k-1. They can be used to help decide the best cutoff of k.

2.7. Statistical analysis

R software was utilized to conduct all statistical analyses. Strawberry Perl was employed to retrieve mRNA expression and mutation profiles for subsequent analyses. The differences in the categorical and continuous variables between the groups were compared via Pearson's chi-square test and the Mann–Whitney *U* test. A two-tailed p or FDR (false discovery rate) $q < 0.05$ indicated a statistically significant difference.

3. Result

3.1. Necroptosis-related signatures identified two HCC subtypes

The gene expression data of 371 HCC patients were obtained from the TCGA database. Unsupervised consensus clustering analysis was utilized to categorize patients according to necroptosis-related gene expression, which demonstrated that the optimum choice was $k = 2$. Therefore, HCC patients from the TCGA database were divided into subtype A (n = 132, 35.6%) and subtype B (n = 239, 64.4%) (Fig. 1A–C). Furthermore, the *t*-SNE analysis demonstrated that the two subtypes could be distinguished clearly (Fig. 1D).

3.2. Association of molecular subtypes with prognosis and clinicopathological features

Kaplan–Meier curves indicated that the patients with subtype B had significantly prolonged survival (Fig. 2A). The differences in demographic and clinical characteristics between the molecular subtypes were compared, and it was found that the patients in subtype A had a higher histologic grade and positive vascular invasion (Table 1 and Fig. 2B). Furthermore, mutational characteristic analysis was performed using somatic mutation data from 361 HCC patients, which showed that the most prevalent mutation among both molecular subtypes was missense mutations (Fig. 3A–B). The horizontal histogram visualized the top 20 mutant genes, showing that TP53 (44.0% vs. 22.6%), FAM47A (6.4% vs. 0.4%), TSC2 (7.2% vs. 1.3%), OBSCN (13.6% vs. 4.8%), and LRP1B (13.6% vs. 5.2%) were mutated more frequently in subtype A, while mutant SPHKAP (0% vs. 3.9%) was more frequent in subtype B (Fig. 3C). Additionally, TTN, CTNNB1, and MUC16 were the most prevalent mutant genes in the two subtypes.

To clarify the potential effect of necroptosis-related classification on the signaling pathway of HCC, we identified 678 differentially expressed genes between HCC subtypes (Supplementary Table S2). Of these, 349 were upregulated in subtype A, and the others were downregulated (Fig. 3D). Functional enrichment analysis showed that several pathways relevant to metabolic processes were significantly enriched in subtype A (such as GO_GLYCINE_METABOLIC_PROCESS and KEGG_RETINOL_METABOLISM), while immune-related or cancer-related pathways (such as GO_ANTIGEN_BINDING and KEGG_PATHWAYS_IN_CANCER) were enriched in subtype B (Fig. 3*E*–F).

ICIs have shown promising efficacy in tumors, including HCC. In addition to immune-related signatures, tumor-infiltrating immune cells and TMB may also be predictive markers of immunotherapy for HCC [27–29] Thus, tumor-infiltrating cells and TMB in the two subtypes were further investigated. For tumor-infiltrating cells, the abundance of B cells, $CD8^+$ T cells, mast cells, plasmacytoid dendritic cells, Th1 cells and Th2 cells was significantly higher in subtype A. However, the abundance of $CD4^+$ T cells, dendritic cells, and regulatory T cells was comparable in the two HCC subtypes (Fig. 4A). Furthermore, the patients in subtype A had a significantly higher TMB (Fig. 4B). Except for PDL1 and CTLA4, other immunosuppression-related genes or immune checkpoint molecules, including LILRB2, LILRB4, NRP1, SIGLEC15, TIM3, and VEGFA, were also significantly upregulated in subtype A (Fig. 4C).

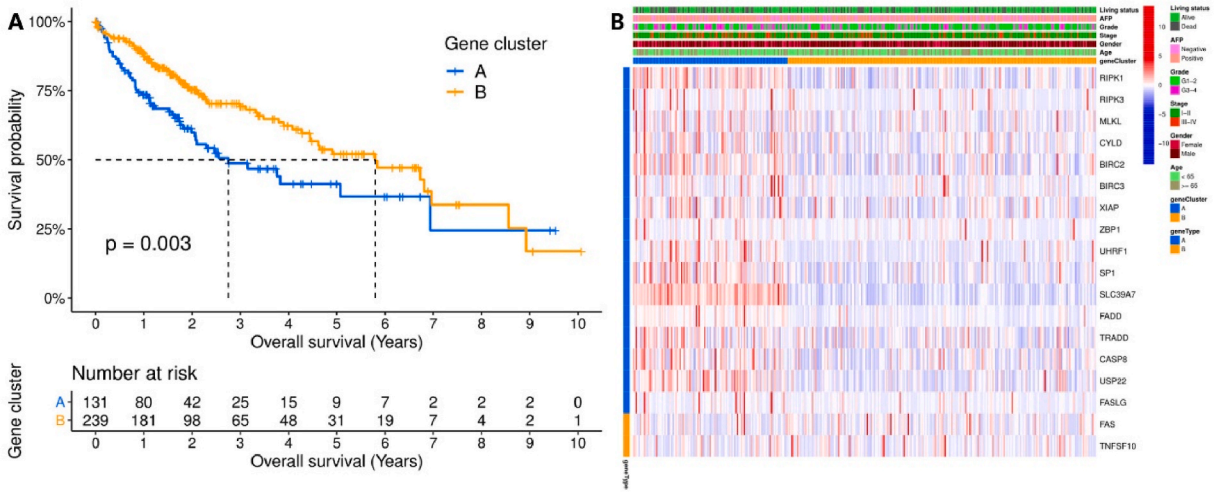

Fig. 2. Association of hepatocellular carcinoma molecular subtypes with survival outcomes. (A) Kaplan–Meier survival curves of the HCC subtypes. (B) Heatmap of necroptosis-related gene expression levels and selected clinicopathological features in each sample.

Table 1
Association of necroptosis-related subtypes with clinicopathological features in HCC patients.

	Subtype			*p*
	Total	A	B	
	(N = 365)	(N = 128)	(N = 237)	
Age (year)				
<65	216 (59.2%)	80 (62.5%)	136 (57.4%)	0.402
≥65	149 (40.8%)	48 (37.5%)	101 (42.6%)	
Gender				
Male	246 (67.4%)	79 (61.7%)	167 (70.5%)	0.113
Female	119 (32.6%)	49 (38.3%)	70 (29.5%)	
Family history of cancer				
Yes	112 (30.7%)	39 (30.5%)	73 (30.8%)	0.916
No	204 (55.9%)	73 (57.0%)	131 (55.3%)	
Unknown	49 (13.4%)	16 (12.5%)	33 (13.9%)	
TNM stage				
I	170 (46.6%)	47 (36.7%)	123 (51.9%)	0.083
II	84 (23.0%)	36 (28.1%)	48 (20.3%)	
III	83 (22.7%)	34 (26.6%)	49 (20.7%)	
IV	4 (1.1%)	1 (0.8%)	3 (1.3%)	
Unknown	24 (6.6%)	10 (7.8%)	14 (5.9%)	
Histologic grade				
G1–2	230 (63.0%)	66 (51.6%)	164 (69.2%)	**0.003**
G3–4	130 (35.6%)	59 (46.1%)	71 (30.0%)	
Unknown	5 (1.4%)	3 (2.3%)	2 (0.8%)	
Ishak score				
0-4	132 (36.2%)	45 (35.2%)	87 (36.7%)	0.165
5-6	77 (21.1%)	21 (16.4%)	56 (23.6%)	
Unknown	156 (42.7%)	62 (48.4%)	94 (39.7%)	
Child-Pugh grade				
A	216 (59.2%)	69 (53.9%)	147 (62.0%)	0.136
B–C	22 (6.0%)	6 (4.7%)	16 (6.8%)	
Unknown	127 (34.8%)	53 (41.4%)	74 (31.2%)	
Vascular invasion				
None	205 (56.2%)	60 (46.9%)	145 (61.2%)	**0.025**
Micro	90 (24.7%)	36 (28.1%)	54 (22.8%)	
Macro	16 (4.4%)	5 (3.9%)	11 (4.6%)	
Unknown	54 (14.8%)	27 (21.1%)	27 (11.4%)	
Alpha fetoprotein				
Positive	275 (75.3%)	103 (80.5%)	172 (72.6%)	0.123
Negative	90 (24.7%)	25 (19.5%)	65 (27.4%)	
Residual tumor				
R0	320 (87.7%)	106 (82.8%)	214 (90.3%)	0.115
R1-2	18 (4.9%)	9 (7.0%)	9 (3.8%)	
Unknown	27 (7.4%)	13 (10.2%)	14 (5.9%)	
Living status				
Alive	235 (64.4%)	73 (57.0%)	162 (68.4%)	**0.041**
Dead	130 (35.6%)	55 (43.0%)	75 (31.6%)	

3.3. Drug sensitivity analysis

Drug sensitivity to immunotherapy, targeted therapy and chemotherapy in HCC subgroups was compared using the TIDE and GDSC databases. The results indicated that HCC patients assigned to subtype B had lower TIDE scores and a desirable immunotherapy response rate (Fig. 5A and B). Moreover, HCC patients assigned to subtype A had lower IC50 values of gemcitabine, etoposide, doxorubicin, rucaparib, and veliparib, while the patients in subtype B had significantly lower IC50 values of docetaxel, dasatinib, erlotinib, gefitinib, and motesanib (Fig. 5C-L). Nevertheless, the estimated IC50 values of cisplatin in the two HCC subtypes were not significantly different (Fig. 5M).

3.4. Necroptosis-related prognostic risk score

The survival data of 365 HCC patients were utilized to determine potential independent prognostic genes from necroptosis-related signatures. After LASSO analysis, nine genes were retained (Fig. 6A–B). According to the results of LASSO analysis, the necroptosis-related prognostic risk score was calculated using nine mRNA expression levels: (0.042570191 × MLKL) + (0.002207222 × FADD) + (0.005074737 × XIAP) + (0.006645083 × USP22) + (0.025310464 × UHRF1) + (0.025523506 × CASP8) + (−0.062858811 × RIPK3) + (−0.018298609 × ZBP1) + (−0.019736246 × FAS). Subsequently, HCC patients from the TCGA database were assigned into high- and low-risk groups based on the optimum cutoff (0.630) for the risk score. As shown in Table 2, sex, family history of cancer, and residual tumor status were not significantly correlated with the necroptosis-related prognostic score.

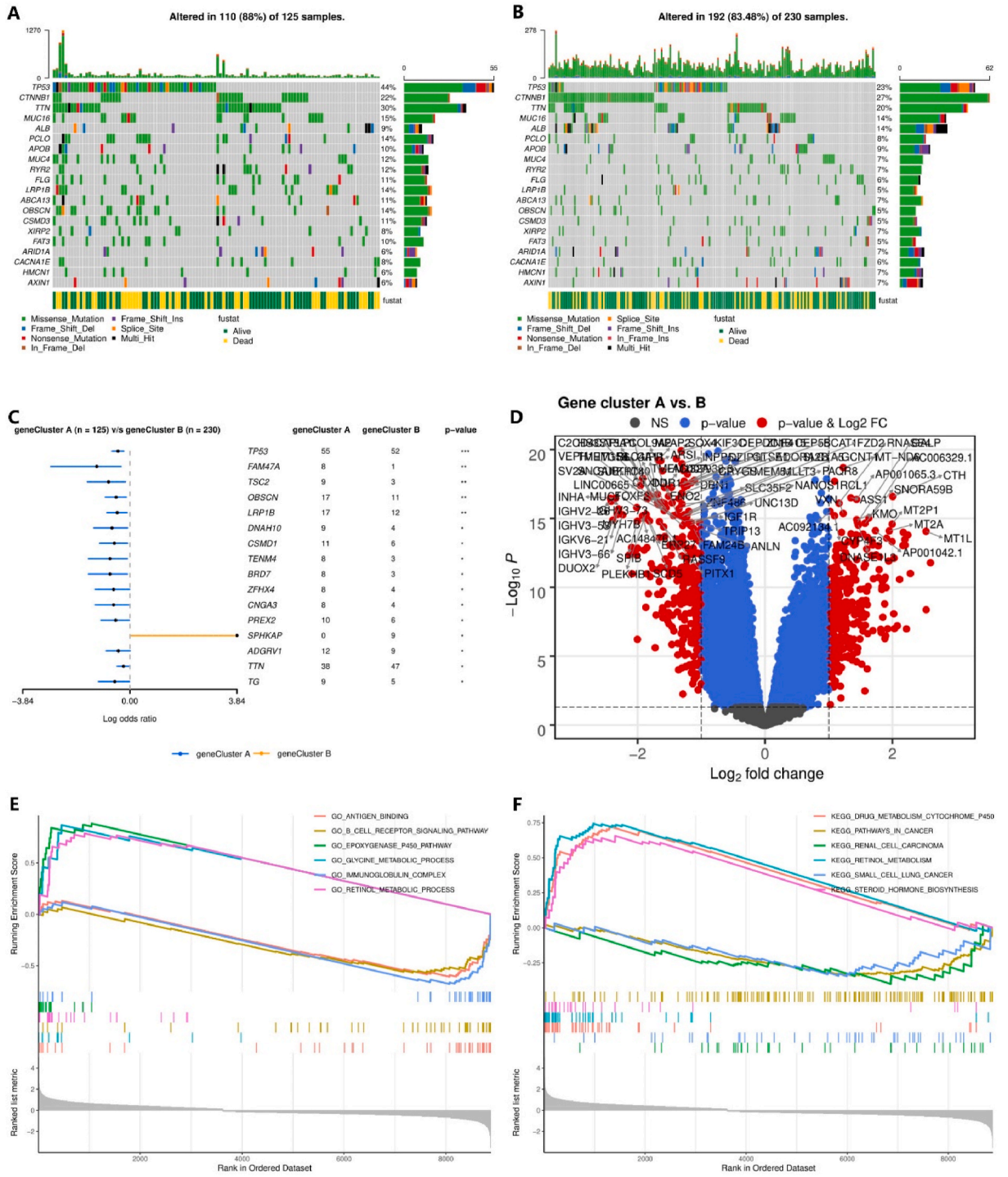

Fig. 3. Differences in mutation characteristics, differentially expressed genes, and enriched pathways between the two hepatocellular carcinoma subtypes. (A, B) Phenotype and distribution of the 20 most prevalent mutant genes in subtypes A and B. (C) The difference in gene mutation frequencies in the two subtypes. (D) The differentially expressed genes in cluster A compared with cluster B. (E, F) GO and KEGG analyses of functional pathways in cluster A compared with cluster B.

Nevertheless, a higher necroptosis-related prognostic score was correlated with advanced TNM stage, higher histologic grade, positive vascular invasion and serum alpha fetoprotein, suggesting that the necroptosis-related risk score may be related to HCC progression. Consistently, Kaplan–Meier curves demonstrated that the patients assigned to the low-risk group had significantly prolonged survival

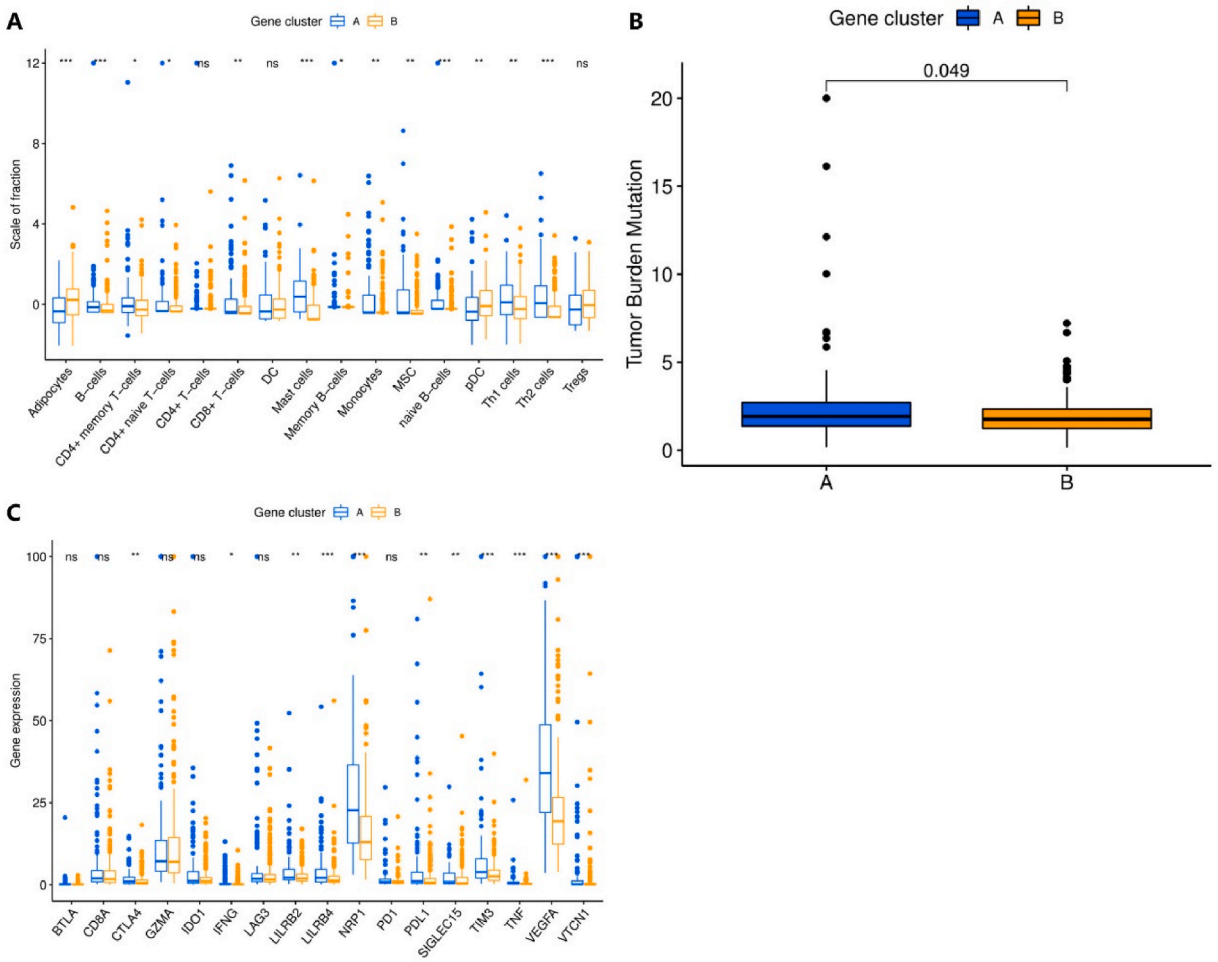

Fig. 4. The difference in infiltrating immune cell abundance, TMB, and immune-related gene expression between the two HCC subtypes. (A) Tumor-infiltrating immune cell abundance, (B) TMB, and (C) the expression of immune-related genes in the two subtypes. TMB, tumor mutation burden. *p < 0.05, **p < 0.01, ***p < 0.001.

(Fig. 7A). Likewise, the prognostic risk score was robust when examined in an external ICGC cohort (Fig. 7B). Moreover, the necroptosis-related prognostic score was positively correlated with the TIDE score (Fig. 7C), suggesting a higher immunotherapy response rate in low-risk patients. On the other hand, when used to predict the OS of HCC patients, the necroptosis-related prognostic risk score constructed in the present study performed better than the well-recognized risk score models developed in the previously published three studies [30–32], both in the TGCA-LIHC and ICGC-LIRI cohorts (Supplementary Figures S1A-S1H).

3.5. Development and assessment of the necroptosis-related prognostic nomogram

As shown in Table 3, univariate Cox analysis demonstrated that vascular invasion status, TNM stage, and necroptosis-related risk score were potential indicators of OS in patients with HCC. Considering that there was no significant difference in OS between patients with TNM stage I and stage II HCC (Table 3), we combined patients with TNM stage I and stage II HCC into one group and performed Cox analysis with the same procedure (Supplementary Table S3). Multivariate Cox analysis identified advanced TNM stage and a higher risk score (HR: 1.98, 95% CI: 1.36–2.87, p < 0.001) as independent predictors of poor OS. Based on multivariate analyses, a prognostic nomogram for HCC patients was developed according to risk score and TNM stage (Fig. 8A). Furthermore, the calibration plot demonstrated that the nomogram had good agreement between the actual and predicted OS (Fig. 8B). The areas under the curve (AUCs) for OS at 1-, 3-, and 5- years were 0.719, 0.737, and 0.719, respectively (Fig. 8C). Ultimately, the DCA curve indicated that the nomogram was more accurate than TNM staging (Fig. 8D).

4. Discussion

The necroptosis-related microenvironment can lead to the transformation from HCC to cholangiocarcinoma, suggesting that

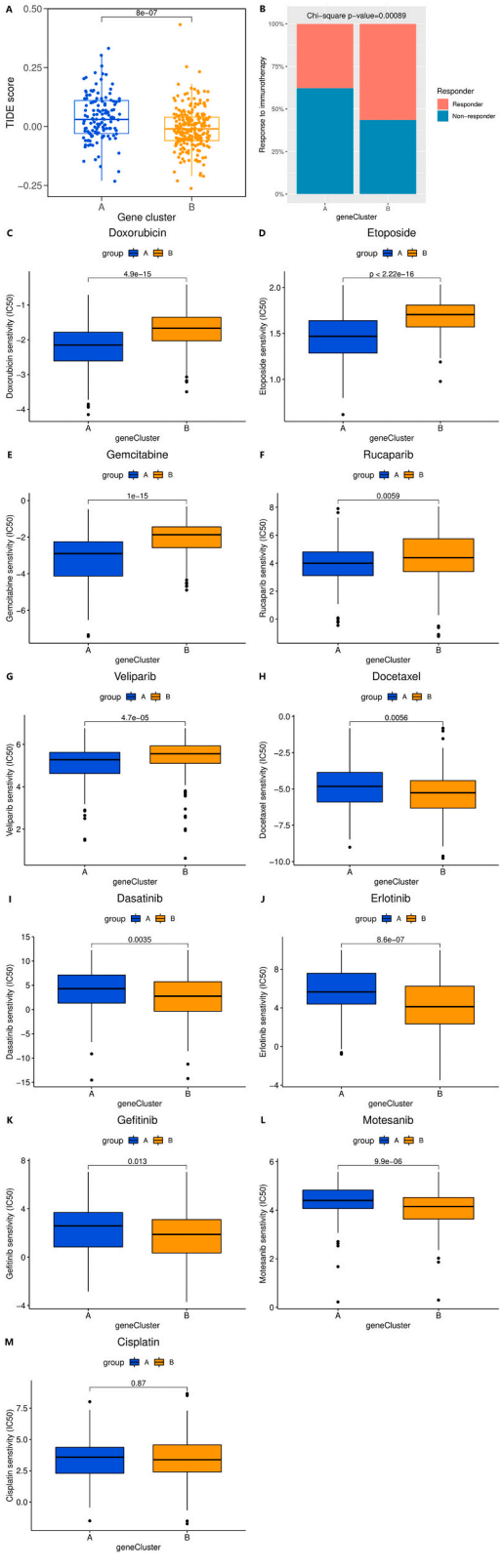

(caption on next page)

Fig. 5. The difference in drug sensitivity between the two molecular subtypes. (A) The difference in the TIDE score. (B) The estimated immunotherapy response rate using the TIDE database in the two subtypes. (C-M) IC50 of targeted therapy or chemotherapy drugs in different subtypes. A lower TIDE score means a higher likelihood of immunotherapy response. The higher the IC50 value is, the lower the drug sensitivity. IC50, half maximal inhibitory concentration.

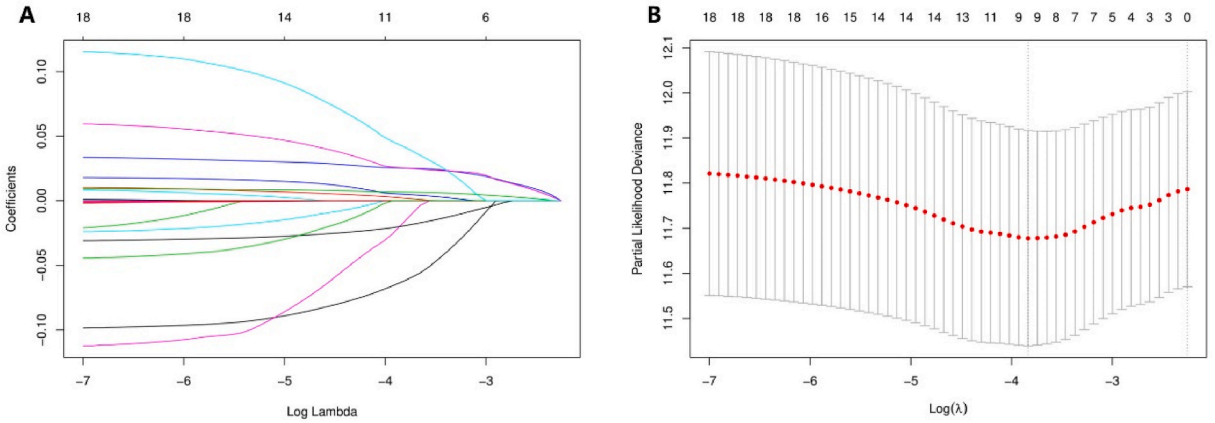

Fig. 6. Determination of potential prognostic genes from necroptosis-related signatures. (A) LASSO coefficient profiles. (B) Screening the best lambda. LASSO, least absolute shrinkage and selection operator.

necroptosis may determine liver cancer lineage commitment [9]. The main mediators of necroptosis include RIPK1, RIPK3, and MLKL [33]. Most HCC cell lines, including Hep3B and HepG2, lose RIPK3 expression and thereby inhibit necroptosis initiation, suggesting that escaping necroptosis is an important process in HCC oncogenesis [7]. HCC is a tumor that generally does not respond to chemotherapy [34]. Nevertheless, restoring RIPK3 expression can enhance the chemosensitivity of HCC cells, suggesting that regulating necroptosis may have the potential to improve sensitivity to chemotherapy [35]. Consistently, necroptosis blockade can lead to sorafenib resistance in HCC [8], while higher expression of necroptosis-related genes is associated with lymphocyte aggregation and longer survival in HCC [11]. These evidences support that, in part, appropriate necroptosis in HCC contributes to eliminating drug-resistant tumor cells and improving patient prognosis. Intriguingly, necroptosis can also contribute to oncogenesis, cancer development, metastasis, and induce inflammatory responses [36]. The role of necroptosis in antitumor immunity is context dependent. The acute and intense necroptosis of cancer cells induced by radiotherapy or chemotherapy is usually immunogenetic, while the mild and spontaneous necroptosis of cancer cells contributes to protumor effects [36]. Considering the effect of necroptosis on hepatic inflammation and fibrosis [37], which is closely linked to liver cancer, it is understandable that necroptosis-related signatures play a vital role in HCC.

In the present research, we demonstrated for the first time that patients with HCC could be classified by necroptosis-related signatures. Survival outcomes in the two HCC subgroups were significantly different, confirming the effect of necroptosis on HCC prognosis. Then, we identified that the patients in subgroup A had a poorer survival outcome, higher histologic grade, and higher mutation frequencies of TP53, FAM47A, TSC2, OBSCN, and LRP1B, while the patients in subgroup B had more mutant SPHKAP. TP53 mutation is believed to be correlated with poor prognosis in various tumors, including HCC [2,38]. TSC2 is a tumor suppressor gene and a potential predictive marker for poor prognosis in HCC [39]. Moreover, LRP1B mutation has been reported to be a marker of unfavorable survival outcomes and poor response to immunotherapy in HCC [40]. SPHKAP mRNA upregulation is related to poor prognosis and higher histologic grade in HCC, but the effect of SPHKAP mutation on HCC has not been identified [41]. Nevertheless, the role of other genes with significantly different mutation rates between subgroup A and subgroup B, such as FAM47A and OBSCN, in tumors has been less studied.

HCC is characterized by angiogenic and inflammatory microenvironments, with heterogeneous sensitivity to immunotherapy and antiangiogenic drugs. Antiangiogenic drugs such as sorafenib have long been the standard treatment for advanced HCC [42]. The IMbrave150 study demonstrated that antiangiogenesis in combination with ICI therapy in the first-line setting could prolong the survival time of HCC patients, but some patients cannot benefit from the combined therapy [29]. Notably, our results showed that HCC patients in necroptosis-related subgroup B, with enriched immune-related pathways, may have a higher likelihood of an ICI response. However, the patients in subtype A were estimated to have a lower immunotherapy response rate, despite having a higher infiltration level of $CD8^+$ T cells. This may be due to the higher expression of immunosuppressive-related genes or immune checkpoint molecules in subtype A, suggesting that the combination of inhibitors targeting different immune checkpoints may be a worthwhile treatment option for patients in subtype A. In addition, multikinase inhibitors against tumor angiogenesis, dasatinib and motesanib, were also estimated to be more effective in subtype B, suggesting that ICI plus antiangiogenesis-based therapy may be an advisable treatment regimen for subtype B patients. Intriguingly, inducing necroptosis may synergize efficiently with immunotherapy and deserves further validation in clinical trials [43,44]. We also noticed that the patients in subtype A had higher expression of VEGFA but higher IC50 values of dasatinib and motesanib. It is necessary to clarify that the VEGFA expression level may not be associated with the efficacy of

Table 2
Association of the necroptosis-related prognostic risk score with clinicopathological features in HCC patients.

	Risk group			*p*
	Total	High	Low	
	(N = 365)	(N = 116)	(N = 249)	
Age (year)				
<65	216 (59.2%)	82 (70.7%)	134 (53.8%)	**0.003**
≥65	149 (40.8%)	34 (29.3%)	115 (46.2%)	
Gender				
Male	246 (67.4%)	70 (60.3%)	176 (70.7%)	0.066
Female	119 (32.6%)	46 (39.7%)	73 (29.3%)	
Family history of cancer				
Yes	112 (30.7%)	28 (24.1%)	84 (33.7%)	0.169
No	204 (55.9%)	72 (62.1%)	132 (53.0%)	
Unknown	49 (13.4%)	16 (13.8%)	33 (13.3%)	
TNM stage				
I	170 (46.6%)	37 (31.9%)	133 (53.4%)	< **0.001**
II	84 (23.0%)	32 (27.6%)	52 (20.9%)	
III	83 (22.7%)	39 (33.6%)	44 (17.7%)	
IV	4 (1.1%)	0 (0%)	4 (1.6%)	
Unknown	24 (6.6%)	8 (6.9%)	16 (6.4%)	
Histologic grade				
G1–2	230 (63.0%)	50 (43.1%)	180 (72.3%)	< **0.001**
G3–4	130 (35.6%)	64 (55.2%)	66 (26.5%)	
Unknown	5 (1.4%)	2 (1.7%)	3 (1.2%)	
Ishak score				
0-4	132 (36.2%)	35 (30.2%)	97 (39.0%)	**0.009**
5-6	77 (21.1%)	18 (15.5%)	59 (23.7%)	
Unknown	156 (42.7%)	63 (54.3%)	93 (37.3%)	
Child-Pugh grade				
A	216 (59.2%)	54 (46.6%)	162 (65.1%)	< **0.001**
B–C	22 (6.0%)	5 (4.3%)	17 (6.8%)	
Unknown	127 (34.8%)	57 (49.1%)	70 (28.1%)	
Vascular invasion				
None	205 (56.2%)	52 (44.8%)	153 (61.4%)	**0.012**
Micro	90 (24.7%)	32 (27.6%)	58 (23.3%)	
Macro	16 (4.4%)	8 (6.9%)	8 (3.2%)	
Unknown	54 (14.8%)	24 (20.7%)	30 (12.0%)	
Alpha fetoprotein				
Positive	275 (75.3%)	96 (82.8%)	179 (71.9%)	**0.035**
Negative	90 (24.7%)	20 (17.2%)	70 (28.1%)	
Residual tumor				
R0	320 (87.7%)	99 (85.3%)	221 (88.8%)	0.648
R1-2	18 (4.9%)	7 (6.0%)	11 (4.4%)	
Unknown	27 (7.4%)	10 (8.6%)	17 (6.8%)	
Living status				
Alive	235 (64.4%)	60 (51.7%)	175 (70.3%)	< **0.001**
Dead	130 (35.6%)	56 (48.3%)	74 (29.7%)	

antiangiogenic drugs [45], but its higher expression predicts a poorer prognosis in patients with HCC [46].

Finally, we constructed a prognostic risk score according to nine necroptosis-related genes (MLKL, FADD, XIAP, USP22, UHRF1, CASP8, RIPK3, ZBP1, and FAS). This is consistent with previous studies showing that higher expression of XIAP, USP22, and UHRF1 is associated with poorer prognosis in HCC [47–49], while the relationship between the rest of the genes and prognosis in HCC has not been determined. Surprisingly, the necroptosis-related prognostic risk score constructed in the present study performed better than the well-recognized risk score models developed in the previously published three studies, which were used to predict postoperative recurrence risk and prognosis [30–32]. Additionally, the necroptosis-related prognostic nomogram showed good agreement between the actual and predicted OS and performed better than TNM staging. Except for use for prognosis evaluation, the necroptosis-related prognostic score was correlated with the TIDE score, supporting the role of necroptosis in cancer immunity.

To date, this is the first study categorizing HCC patients according to necroptosis-related signatures. Moreover, a necroptosis-related prognostic risk score and nomogram were constructed and validated. These results confirmed the important role of necroptosis in HCC and can aid in clinical decision making and prognostic prediction. For example, patients classified as subgroup A with worse prognosis may prefer a more aggressive chemotherapy regimen over immunotherapy. Nevertheless, some limitations of this research need to be pointed out. First, this study was retrospective, in which the inherent confounding bias is almost inevitable, and the causal relationship between gene expression and prognosis could not be determined. Hence, validation using prospective trials and preclinical experiments is warranted. Second, we failed to analyze the sensitivity of some important drugs for HCC, including lenvatinib, which may be settled in vitro and in vivo experiments. Third, given that proteins are the executors of cellular functions, necroptosis is also induced based on protein signaling. Despite the lack of a highly specific marker for necroptosis

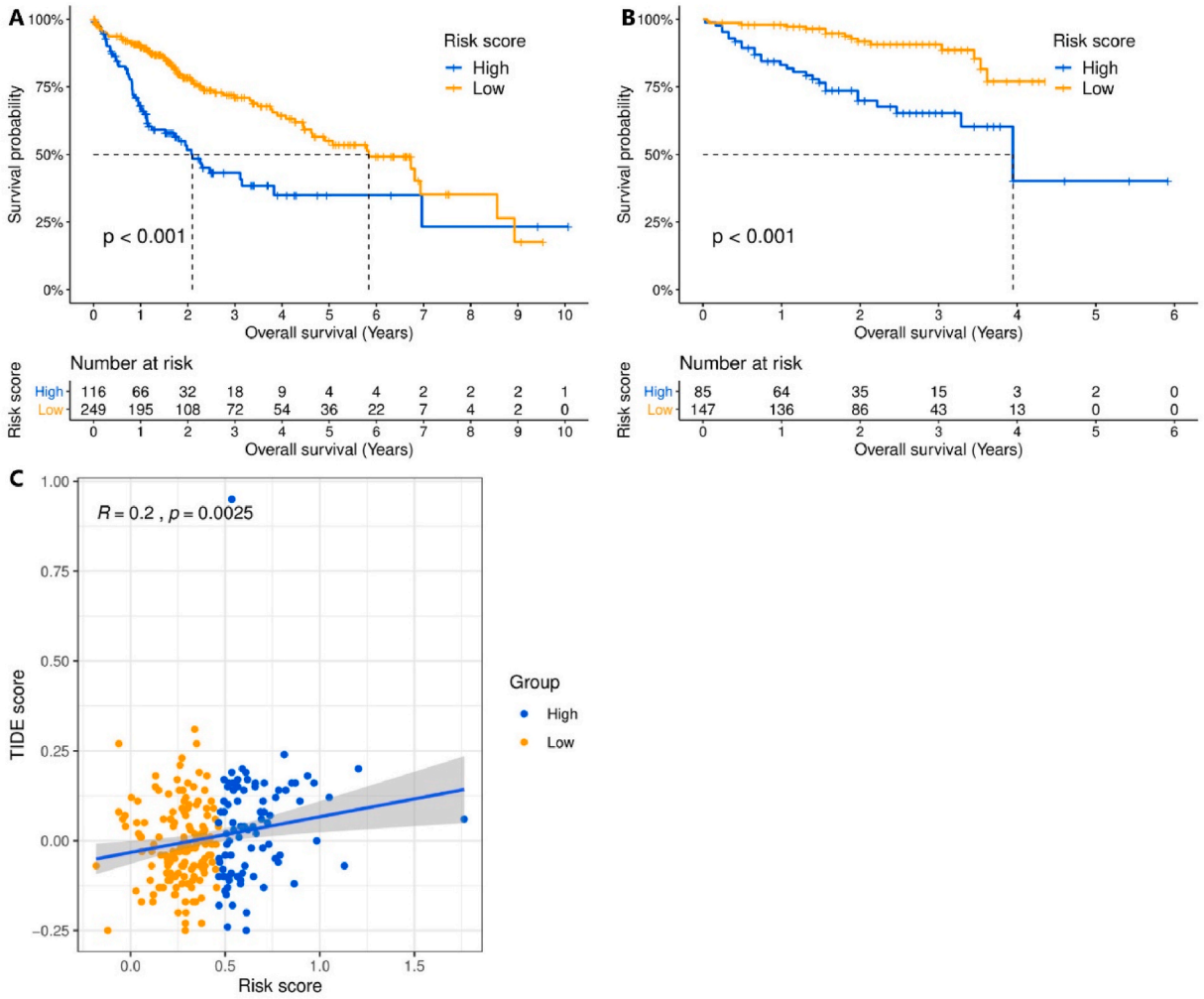

Fig. 7. Estimating the necroptosis-related prognostic risk score in cohorts. (A) TCGA-LIHC dataset. (B) ICGC-LIRI dataset. (C) Correlation analysis between the TIDE score and the necroptosis-related prognostic score.

Table 3
Cox analyses of overall survival.

Variables	Univariate analysis		Multivariate analysis	
	HR (95% CI)	*p*	HR (95% CI)	*p*
Age (≥65 vs.<65)	1.24 (0.88,1.75)	0.228	–	–
Gender (Male vs. Female)	0.82 (0.57,1.16)	0.260	–	–
Family history of cancer (Yes vs. No)	1.18 (0.82,1.70)	0.382	–	–
TNM stage (II vs. I)	1.43 (0.88,2.34)	0.151	1.25 (0.72,2.19)	0.427
TNM stage (III vs. I)	2.72 (1.78,4.15)	< **0.001**	1.85 (1.15,2.98)	**0.012**
TNM stage (IV vs. I)	5.79 (1.78,18.78)	**0.003**	7.41 (2.27,24.22)	**0.001**
Histologic grade (G3–4 vs. G1–2)	1.12 (0.78,1.61)	0.528	–	–
Ishak score (5–6 vs. 0–4)	0.82 (0.48,1.40)	0.464	–	–
Child-Pugh grade (B–C vs. A)	1.63 (0.81,3.30)	0.173	–	–
Vascular invasion (Micro vs. None)	1.21 (0.77,1.89)	0.411	1.08 (0.65,1.80)	0.768
Vascular invasion (Macro vs. None)	2.21 (1.05,4.65)	**0.036**	1.49 (0.69,3.26)	0.313
Alpha fetoprotein (Positive vs. Negative)	1.27 (0.84,1.92)	0.264	–	–
Residual tumor (R1–2 vs. R0)	1.57 (0.80,3.11)	0.191	–	–
Risk score (High vs. Low)	2.33 (1.64,3.31)	< **0.001**	1.94 (1.33,2.82)	**0.001**

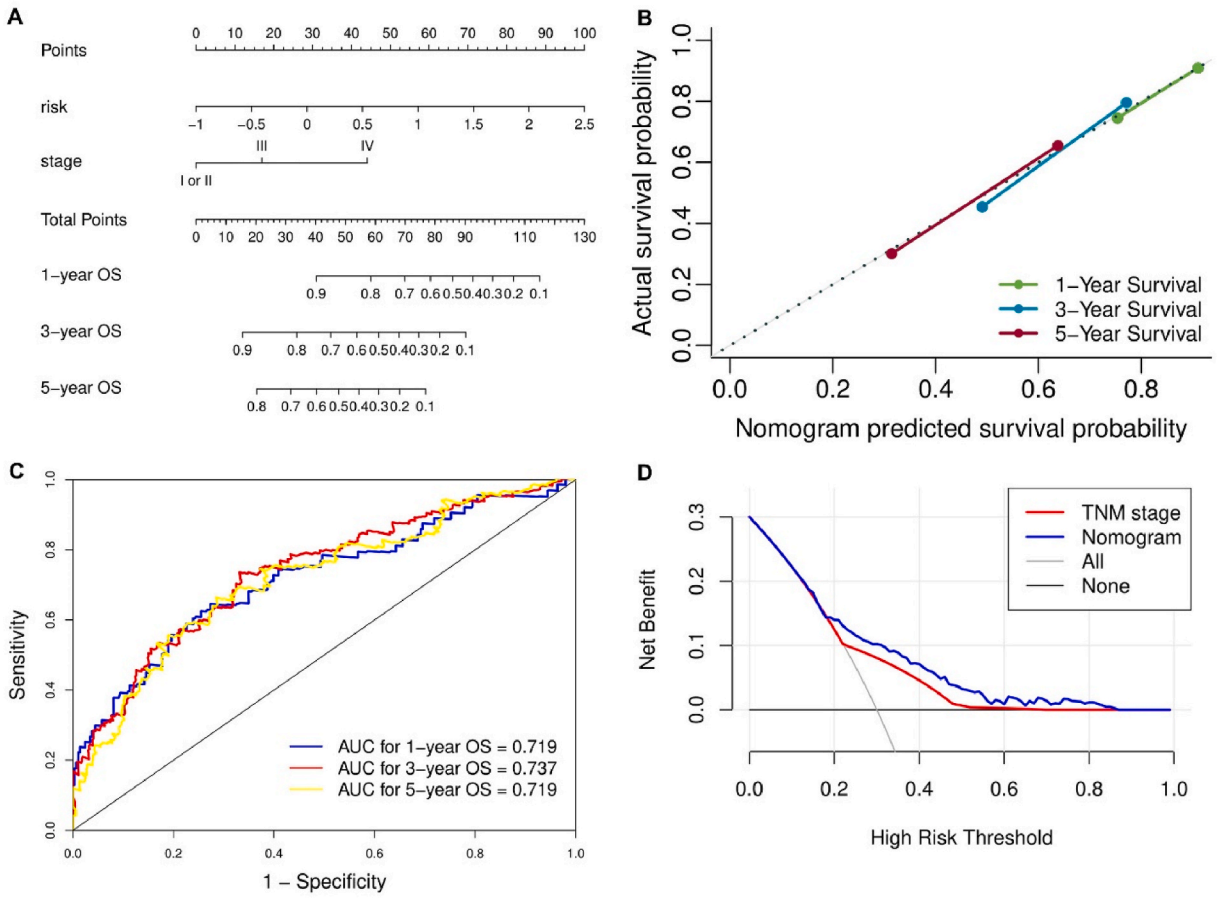

Fig. 8. Evaluation of the necroptosis-related prognostic nomogram model. (A) The nomogram used for anticipating overall survival in HCC patients. (B) The calibration curves. (C) The receiver operating characteristic curves. (D) The decision curve analysis. Net benefit means true positives minus false positives (after multiplied by an "exchange rate" to place it on the same scale as true positives), the higher the net benefit, the better the model predicts.

immunohistochemical analysis, further proteomic studies are also needed to assess the effect of necroptosis on HCC. Nonetheless, many previous studies have also focused on necroptosis at the transcriptome level. Meanwhile, necroptosis-related signatures demonstrate good accuracy in prognosis evaluation and provide abundant information about the HCC microenvironment, suggesting that it is rational to analyze the role of necroptosis in HCC based on necroptosis-related mRNA signatures.

5. Conclusion

In conclusion, based on necroptosis-related signatures, two HCC subtypes were identified with different mutation characteristics, drug sensitivities, and survival outcomes. Additionally, a necroptosis-related prognostic model was constructed and validated. Our findings add to the growing evidence supporting the role of necroptosis-related signatures in HCC and are worth being fully elucidated and validated.

Ethics statement

The need for further ethics approval was waived by The Medical Ethics Committee of Peking Union Medical College Hospital, because the data downloaded from public databases are deidentified.

Funding statement

This study was supported by National High Level Hospital Clinical Research Funding (2022-PUMCH-A-213, 2022-PUMCH-D-001, 2022-PUMCH-A-126).

Data availability statement

The datasets used in this study can be retrieved from the online repositories mentioned in the text.

Authors' contributions

HT, SZ, CB and YW conceived and designed the experiments. HT, RG and CQ performed the experiments. HT, CQ, ZG, SZ, CB and YW analyzed and interpreted the data. HT, CQ and ZG contributed reagents, materials, analysis tools or data. HT, CQ, ZG, RG, SZ, CB and YW wrote the paper.

Declaration of competing interest

The authors declare that they have no known competing financial interests or personal relationships that could have appeared to influence the work reported in this paper.

Appendix A. Supplementary data

Supplementary data to this article can be found online at https://doi.org/10.1016/j.heliyon.2023.e18136.

References

[1] F. Bray, J. Ferlay, I. Soerjomataram, R.L. Siegel, L.A. Torre, A. Jemal, Global cancer statistics 2018: GLOBOCAN estimates of incidence and mortality worldwide for 36 cancers in 185 countries, CA A Cancer J. Clin. 68 (6) (2018) 394–424, https://doi.org/10.3322/caac.21492.
[2] A. Villanueva, Hepatocellular carcinoma, N. Engl. J. Med. 380 (15) (2019) 1450–1462, https://doi.org/10.1056/NEJMra1713263.
[3] A. Degterev, Z. Huang, M. Boyce, Y. Li, P. Jagtap, N. Mizushima, et al., Chemical inhibitor of nonapoptotic cell death with therapeutic potential for ischemic brain injury, Nat. Chem. Biol. 1 (2) (2005) 112–119, https://doi.org/10.1038/nchembio711.
[4] J. Yan, P. Wan, S. Choksi, Z.G. Liu, Necroptosis and tumor progression, Trends Cancer 8 (1) (2022) 21–27, https://doi.org/10.1016/j.trecan.2021.09.003.
[5] A. Negroni, E. Colantoni, S. Cucchiara, L. Stronati, Necroptosis in intestinal inflammation and cancer: new concepts and therapeutic perspectives, Biomolecules 10 (10) (2020), https://doi.org/10.3390/biom10101431.
[6] T. Luedde, N. Kaplowitz, R.F. Schwabe, Cell death and cell death responses in liver disease: mechanisms and clinical relevance, Gastroenterology 147 (4) (2014) 765–783.e764, https://doi.org/10.1053/j.gastro.2014.07.018.
[7] X. Li, G. Dong, H. Xiong, H. Diao, A narrative review of the role of necroptosis in liver disease: a double-edged sword, Ann. Transl. Med. 9 (5) (2021) 422, https://doi.org/10.21037/atm-20-5162.
[8] Y. Liao, Y. Yang, D. Pan, Y. Ding, H. Zhang, Y. Ye, et al., HSP90α mediates sorafenib resistance in human hepatocellular carcinoma by necroptosis inhibition under hypoxia, Cancers 13 (2) (2021), https://doi.org/10.3390/cancers13020243.
[9] M. Seehawer, F. Heinzmann, L. D'Artista, J. Harbig, P.F. Roux, L. Hoenicke, et al., Necroptosis microenvironment directs lineage commitment in liver cancer, Nature 562 (7725) (2018) 69–75, https://doi.org/10.1038/s41586-018-0519-y.
[10] A.T. Schneider, J. Gautheron, M. Feoktistova, C. Roderburg, S.H. Loosen, S. Roy, et al., RIPK1 suppresses a TRAF2-dependent pathway to liver cancer, Cancer Cell 31 (1) (2017) 94–109, https://doi.org/10.1016/j.ccell.2016.11.009.
[11] L. Nicolè, T. Sanavia, R. Cappellesso, V. Maffeis, J. Akiba, A. Kawahara, et al., Necroptosis-driving genes RIPK1, RIPK3 and MLKL-p are associated with intratumoral CD3(+) and CD8(+) T cell density and predict prognosis in hepatocellular carcinoma, J. Immunother. Cancer 10 (3) (2022), https://doi.org/10.1136/jitc-2021-004031.
[12] G.P. Wagner, K. Kin, V.J. Lynch, Measurement of mRNA abundance using RNA-seq data: RPKM measure is inconsistent among samples, Theor. Biosci. 131 (4) (2012) 281–285, https://doi.org/10.1007/s12064-012-0162-3.
[13] A. Najafov, H. Chen, J. Yuan, Necroptosis and cancer, Trends Cancer 3 (4) (2017) 294–301, https://doi.org/10.1016/j.trecan.2017.03.002.
[14] C. Yang, J. Li, L. Yu, Z. Zhang, F. Xu, L. Jiang, et al., Regulation of RIP3 by the transcription factor Sp1 and the epigenetic regulator UHRF1 modulates cancer cell necroptosis, Cell Death Dis. 8 (10) (2017), e3084, https://doi.org/10.1038/cddis.2017.483.
[15] Y. Gong, Z. Fan, G. Luo, C. Yang, Q. Huang, K. Fan, et al., The role of necroptosis in cancer biology and therapy, Mol. Cancer 18 (1) (2019) 100, https://doi.org/10.1186/s12943-019-1029-8.
[16] A. Fauster, M. Rebsamen, K.L. Willmann, A. César-Razquin, E. Girardi, J.W. Bigenzahn, et al., Systematic genetic mapping of necroptosis identifies SLC39A7 as modulator of death receptor trafficking, Cell Death Differ. 26 (6) (2019) 1138–1155, https://doi.org/10.1038/s41418-018-0192-6.
[17] J. Roedig, L. Kowald, T. Juretschke, R. Karlowitz, B. Ahangarian Abhari, H. Roedig, et al., USP22 controls necroptosis by regulating receptor-interacting protein kinase 3 ubiquitination, EMBO Rep. 22 (2) (2021), e50163, https://doi.org/10.15252/embr.202050163.
[18] M.D. Wilkerson, D.N. Hayes, ConsensusClusterPlus: a class discovery tool with confidence assessments and item tracking, Bioinformatics 26 (12) (2010) 1572–1573, https://doi.org/10.1093/bioinformatics/btq170.
[19] V.D.M. Laurens, Accelerating t-SNE using tree-based algorithms, J. Mach. Learn. Res. 15 (1) (2014) 3221–3245.
[20] A. Mayakonda, D.C. Lin, Y. Assenov, C. Plass, H.P. Koeffler, Maftools: efficient and comprehensive analysis of somatic variants in cancer, Genome Res. 28 (11) (2018) 1747–1756, https://doi.org/10.1101/gr.239244.118.
[21] D. Aran, Z. Hu, A.J. Butte, xCell: digitally portraying the tissue cellular heterogeneity landscape, Genome Biol. 18 (1) (2017) 220, https://doi.org/10.1186/s13059-017-1349-1.
[22] G. Yu, L.G. Wang, Y. Han, Q.Y. He, clusterProfiler: an R package for comparing biological themes among gene clusters, OMICS 16 (5) (2012) 284–287, https://doi.org/10.1089/omi.2011.0118.
[23] P. Jiang, S. Gu, D. Pan, J. Fu, A. Sahu, X. Hu, et al., Signatures of T cell dysfunction and exclusion predict cancer immunotherapy response, Nat. Med. 24 (10) (2018) 1550–1558, https://doi.org/10.1038/s41591-018-0136-1.
[24] W. Yang, J. Soares, P. Greninger, E.J. Edelman, H. Lightfoot, S. Forbes, et al., Genomics of Drug Sensitivity in Cancer (GDSC): a resource for therapeutic biomarker discovery in cancer cells, Nucleic Acids Res. 41 (Database issue) (2013) D955–D961, https://doi.org/10.1093/nar/gks1111.
[25] P. Geeleher, N. Cox, R.S. Huang, pRRophetic: an R package for prediction of clinical chemotherapeutic response from tumor gene expression levels, PLoS One 9 (9) (2014), e107468, https://doi.org/10.1371/journal.pone.0107468.
[26] J. Friedman, T. Hastie, R. Tibshirani, Regularization paths for generalized linear models via coordinate descent, J. Stat. Software 33 (1) (2010) 1–22.

[27] Y. Dai, W. Qiang, K. Lin, Y. Gui, X. Lan, D. Wang, An immune-related gene signature for predicting survival and immunotherapy efficacy in hepatocellular carcinoma, Cancer Immunol. Immunother. 70 (4) (2021) 967–979, https://doi.org/10.1007/s00262-020-02743-0.
[28] W. Hong, L. Liang, Y. Gu, Z. Qi, H. Qiu, X. Yang, et al., Immune-related lncRNA to construct novel signature and predict the immune landscape of human hepatocellular carcinoma, Mol. Ther. Nucleic Acids 22 (2020) 937–947, https://doi.org/10.1016/j.omtn.2020.10.002.
[29] M. Pinter, R.K. Jain, D.G. Duda, The current landscape of immune checkpoint blockade in hepatocellular carcinoma: a review, JAMA Oncol. 7 (1) (2021) 113–123, https://doi.org/10.1001/jamaoncol.2020.3381.
[30] J.Y. Liang, D.S. Wang, H.C. Lin, X.X. Chen, H. Yang, Y. Zheng, et al., A novel ferroptosis-related gene signature for overall survival prediction in patients with hepatocellular carcinoma, Int. J. Biol. Sci. 16 (13) (2020) 2430–2441, https://doi.org/10.7150/ijbs.45050.
[31] Y. Tang, L. Xu, Y. Ren, Y. Li, F. Yuan, M. Cao, et al., Identification and validation of a prognostic model based on three MVI-related genes in hepatocellular carcinoma, Int. J. Biol. Sci. 18 (1) (2022) 261–275, https://doi.org/10.7150/ijbs.66536.
[32] S.M. Kim, S.H. Leem, I.S. Chu, Y.Y. Park, S.C. Kim, S.B. Kim, et al., Sixty-five gene-based risk score classifier predicts overall survival in hepatocellular carcinoma, Hepatology 55 (5) (2012) 1443–1452, https://doi.org/10.1002/hep.24813.
[33] J. Sprooten, P. De Wijngaert, I. Vanmeerbeerk, S. Martin, P. Vangheluwe, S. Schlenner, et al., Necroptosis in immuno-oncology and cancer immunotherapy, Cells 9 (8) (2020), https://doi.org/10.3390/cells9081823.
[34] G.L. Deng, S. Zeng, H. Shen, Chemotherapy and target therapy for hepatocellular carcinoma: new advances and challenges, World J. Hepatol. 7 (5) (2015) 787–798, https://doi.org/10.4254/wjh.v7.i5.787.
[35] G.B. Koo, M.J. Morgan, D.G. Lee, W.J. Kim, J.H. Yoon, J.S. Koo, et al., Methylation-dependent loss of RIP3 expression in cancer represses programmed necrosis in response to chemotherapeutics, Cell Res. 25 (6) (2015) 707–725, https://doi.org/10.1038/cr.2015.56.
[36] W. Chen, W. Lin, L. Wu, A. Xu, C. Liu, P. Huang, A novel prognostic predictor of immune microenvironment and therapeutic response in kidney renal clear cell carcinoma based on necroptosis-related gene signature, Int. J. Med. Sci. 19 (2) (2022) 377–392, https://doi.org/10.7150/ijms.69060.
[37] S. Mohammed, E.H. Nicklas, N. Thadathil, R. Selvarani, G.H. Royce, M. Kinter, et al., Role of necroptosis in chronic hepatic inflammation and fibrosis in a mouse model of increased oxidative stress, Free Radic. Biol. Med. 164 (2021) 315–328, https://doi.org/10.1016/j.freeradbiomed.2020.12.449.
[38] M. Olivier, M. Hollstein, P. Hainaut, TP53 mutations in human cancers: origins, consequences, and clinical use, Cold Spring Harbor Perspect. Biol. 2 (1) (2010) a001008, https://doi.org/10.1101/cshperspect.a001008.
[39] Q.Y. Zhu, Z.M. He, W.M. Cao, B. Li, The role of TSC2 in breast cancer: a literature review, Front. Oncol. 13 (2023), 1188371, https://doi.org/10.3389/fonc.2023.1188371.
[40] Y. Cheng, R. Tang, X. Li, B. Wang, Y. Cheng, S. Xiao, et al., LRP1B is a potential biomarker for tumor immunogenicity and prognosis of HCC patients receiving ICI treatment, J. Hepatocell. Carcinoma 9 (2022) 203–220, https://doi.org/10.2147/jhc.S348785.
[41] G. Liu, X. Huang, X. Cui, J. Zhang, L. Wei, R. Ni, et al., High SKIP expression is correlated with poor prognosis and cell proliferation of hepatocellular carcinoma, Med. Oncol. 30 (3) (2013) 537, https://doi.org/10.1007/s12032-013-0537-4.
[42] J.M. Llovet, S. Ricci, V. Mazzaferro, P. Hilgard, E. Gane, J.F. Blanc, et al., Sorafenib in advanced hepatocellular carcinoma, N. Engl. J. Med. 359 (4) (2008) 378–390, https://doi.org/10.1056/NEJMoa0708857.
[43] S.T. Workenhe, A. Nguyen, D. Bakhshinyan, J. Wei, D.N. Hare, K.L. MacNeill, et al., De novo necroptosis creates an inflammatory environment mediating tumor susceptibility to immune checkpoint inhibitors, Commun. Biol. 3 (1) (2020) 645, https://doi.org/10.1038/s42003-020-01362-w.
[44] L. Van Hoecke, S. Van Lint, K. Roose, A. Van Parys, P. Vandenabeele, J. Grooten, et al., Treatment with mRNA coding for the necroptosis mediator MLKL induces antitumor immunity directed against neo-epitopes, Nat. Commun. 9 (1) (2018) 3417, https://doi.org/10.1038/s41467-018-05979-8.
[45] C. Bais, C. Rabe, N. Wild, M. Swiatek-de Lange, D. Chen, K. Hong, et al., Comprehensive reassessment of plasma VEGFA (pVEGFA) as a candidate predictive biomarker for bevacizumab (Bv) in 13 pivotal trials (seven indications), J. Clin. Oncol. 32 (15_suppl) (2014) 3040, https://doi.org/10.1200/jco.2014.32.15_suppl.3040.
[46] J.M. Llovet, C.E. Peña, C.D. Lathia, M. Shan, G. Meinhardt, J. Bruix, Plasma biomarkers as predictors of outcome in patients with advanced hepatocellular carcinoma, Clin. Cancer Res. 18 (8) (2012) 2290–2300, https://doi.org/10.1158/1078-0432.Ccr-11-2175.
[47] B. Tang, X. Liang, F. Tang, J. Zhang, S. Zeng, S. Jin, et al., Expression of USP22 and Survivin is an indicator of malignant behavior in hepatocellular carcinoma, Int. J. Oncol. 47 (6) (2015) 2208–2216, https://doi.org/10.3892/ijo.2015.3214.
[48] R. Mudbhary, Y. Hoshida, Y. Chernyavskaya, V. Jacob, A. Villanueva, M.I. Fiel, et al., UHRF1 overexpression drives DNA hypomethylation and hepatocellular carcinoma, Cancer Cell 25 (2) (2014) 196–209, https://doi.org/10.1016/j.ccr.2014.01.003.
[49] W. Lou, J. Chen, B. Ding, W. Fan, XIAP, commonly targeted by tumor suppressive miR-3607-5p and miR-3607-3p, promotes proliferation and inhibits apoptosis in hepatocellular carcinoma, Genomics 113 (3) (2021) 933–945, https://doi.org/10.1016/j.ygeno.2021.02.003.